JPET Fast Forward. Published on May 16, 2011 as DOI: 10.1124/jpet.111.180521

TITLE PAGE

The Role of Hypoxia Inducible Factor-1 alpha (HIF-1α) in Acetaminophen Hepatotoxicity

Erica M. Sparkenbaugh

Yogesh Saini

Krista K. Greenwood

John J. LaPres

James P. Luyendyk

Bryan L. Copple

Jane F. Maddox

Patricia E. Ganey

Robert A. Roth

Department of Pharmacology and Toxicology, Michigan State University – EMS, JFM, PEG, RAR

Department of Biochemistry and Molecular Biology, Michigan State University – EMS, YS, KKG, JJL, PEG, RAR

Center for Integrative Toxicology, Michigan State University YS, KKG, JJL, JFM, PEG, RAR

Department of Pharmacology, Toxicology and Therapeutics, University of Kansas Medical Center, JPL, BLC

RUNNING TITLE PAGE

a) Running Title: Role of HIF-1α in Acetaminophen Hepatotoxicity

b) Corresponding Author

Robert A. Roth, PhD, DABT
221 Food Safety and Toxicology Center
Michigan State University
East Lansing, MI 48824
rothr@msu.edu
Phone: 517-353-9841
Fax: 517-432-2310

c) Number of Text Pages: 19
Number of Tables: 4
Number of Figures: 9
Number of References: 44
Number of Words (Abstract): 239
Number of Words (Introduction): 720
Number of Words (Discussion): 1420

d) Nonstandard Abbreviations

ALT – alanine aminotransferase
APAP – *N*-acetyl-*p*-aminophenol
HIF – hypoxia inducible factor
IL – interleukin
KC – keratinocyte chemoattractant
NAPQI – *n*-acetyl-*p*-benzoquinone imine
PAI-1 – plasminogen activator inhibitor-1
PMN - polymorphonuclear lymphocyte, or neutrophil
RANTES - regulated upon activation normal T cell expressed and excreted
ROS – reactive oxygen species
TAM – tamoxifen
TF - Tissue Factor
TNF – tumor necrosis factor
VEGF – vascular endothelial growth factor

e) Recommended section: Toxicology

JPET Fast Forward. Published on May 16, 2011 as DOI: 10.1124/jpet.111.180521
This article has not been copyedited and formatted. The final version may differ from this version.

ABSTRACT

Hypoxia inducible factor-1 alpha (HIF-1α) is a critical transcription factor that controls oxygen homeostasis in response to hypoxia, inflammation and oxidative stress. HIF has been implicated in the pathogenesis of liver injury in which these events play a role, including acetaminophen (APAP) overdose, which is the leading cause of acute liver failure in the US. APAP overdose has been reported to activate HIF-1α in mouse livers and isolated hepatocytes downstream of oxidative stress. HIF-1α signaling controls many factors that contribute to APAP hepatotoxicity, including mitochondrial cell death, inflammation, and hemostasis. Therefore, we tested the hypothesis that HIF-1α contributes to APAP hepatotoxicity. Conditional HIF-1α deletion was generated in mice using an inducible Cre-lox system. Control (HIF-1α-sufficient) mice developed severe liver injury 6 and 24h after APAP overdose (400 mg/kg). HIF-1α-deficient mice were protected from APAP hepatotoxicity at 6h, but developed severe liver injury by 24h, suggesting that HIF-1α is involved in the early stage of APAP toxicity. In further studies, HIF-1α-deficient mice had attenuated thrombin generation and reduced plasminogen activator inhibitor-1 (PAI-1) production compared to control mice, indicating that HIF-1α signaling contributes to hemostasis in APAP hepatotoxicity. Finally, HIF-1α-deficient animals had decreased hepatic neutrophil accumulation and plasma concentrations of interleukin-6 (IL-6), keratinocyte chemoattractant (KC) and regulated upon activation normal T cell expressed and excreted (RANTES) compared to control mice, suggesting an altered inflammatory response. HIF-1α contributes to hemostasis, sterile inflammation, and early hepatocellular necrosis during the pathogenesis of APAP toxicity.

INTRODUCTION

Hypoxia inducible factor (HIF) is the master regulator of oxygen homeostasis. It controls the expression of a large battery of genes involved in angiogenesis, erythropoiesis, glycolysis, inflammation, and cell death (Lee et al., 2007). HIF comprises two constitutively expressed subunits: HIF-1α and HIF-1β. HIF-1α is primarily regulated at the level of protein stability: at normal oxygen tension, oxygen-dependent proline hydroxylation of HIF-1α targets it for rapid proteasomal degradation. In hypoxia, decreased proline hydroxylation causes HIF-1α to accumulate and translocate to the nucleus, where it binds to HIF-1β, forming the transcriptionally competent HIF-1 that binds hypoxia response elements in DNA. HIF-regulated genes include plasminogen activator inhibitor-1 (PAI-1), vascular endothelial growth factor (VEGF), tumor necrosis factor alpha (TNFα), interleukin-1 beta (IL-1β), and cell death proteins such as BNIP3 and Nix (Murdoch et al., 2005; Lee et al., 2007). HIF-1α expression and activation are also regulated by oxidative stress (Klimova and Chandel, 2008), inflammatory cytokines (Walmsley et al., 2005a) and thrombin (Gorlach et al., 2001). Due to the many factors that can modulate HIF induction and the variety of downstream signaling targets, HIF has been identified as a key regulator of a generalized stress response (James et al., 2006).

HIF-1α has been implicated in hepatocyte death in models of liver injury that have an inflammatory or oxidative stress component, such as sepsis (Peyssonnaux et al., 2007), ischemia/reperfusion (Cursio et al., 2008), alcoholic liver disease (Li et al., 2006) and fibrosis (Copple et al., 2009). Oxidative stress and mitochondrial dysfunction play a key role in acetaminophen (*N*-acetyl-*p*-aminophenol, [APAP])-induced liver injury. APAP overdose is the leading cause of drug-induced liver failure in the United States (Lee, 2007). At toxic doses, APAP is bioactivated by cytochrome P450 enzymes to *n*-acetyl-*p*-benzoquinone imine (NAPQI), which is reactive, depletes glutathione (GSH) and binds covalently to intracellular proteins, leading to mitochondrial dysfunction, production of reactive oxygen species (ROS) and hepatocellular necrosis (Jollow et al., 1973).

Recent reports by James *et al.* (2006) indicated that APAP overdose causes nuclear accumulation of HIF-1α in mouse livers as early as 1h after treatment, which is before the onset of liver hypoxia and hepatocellular injury. Furthermore, N-acetyl cysteine, which inactivates NAPQI (James et al., 2006) or cyclosprin A, which prevents mitochondrial permeability transition (MPT) prevented HIF-1α accumulation (Chaudhuri et al., 2011). Taken together, these data suggest that mitochondrial dysfunction and ROS are important contributors to early HIF-1α stabilization in APAP overdose.

In addition to cellular necrosis caused by oxidative stress and mitochondrial dysfunction, APAP hepatotoxicity is also associated with disturbances to the hemostatic system in humans (James, et al., 2002) and experimental animals (Ganey et al., 2007). APAP overdose caused tissue factor-dependent activation of the coagulation system in mice, elevated circulating concentration of PAI-1 and fibrin deposition in liver (Ganey et al., 2007). Inhibition of coagulation system activation through genetic or pharmacologic methods attenuated APAP-induced liver injury, suggesting a role for thrombin and the coagulation system in the pathogenesis. During injury progression, fibrin deposition can contribute to tissue ischemia and hypoxia, which might enhance HIF-1α accumulation above that caused by oxidative stress alone.

APAP hepatotoxicity is accompanied by a sterile inflammatory response (Williams et al., 2010), and concurrent inflammation can sensitize mice to APAP-induced liver injury (Maddox et al., 2010). Mediators released from necrotic hepatocytes activate Kupffer cells, recruit and activate neutrophils (PMNs), and consequently produce cytokines that influence APAP-induced hepatocellular injury (James et al., 2005; Cover et al., 2006). The role of PMNs in APAP hepatotoxicity remains controversial, with evidence both for and against a contribution of PMNs to injury progression (Jaeschke, 2008). HIF-1α plays a critical role in PMN function; it influences phagocytosis, motility, invasiveness, and apoptosis (Cramer et al., 2003; Peyssonnaux et al., 2005; Walmsley et al., 2005a; Walmsley et al., 2005b). HIF-1α also contributes to inflammatory cytokine production (Zinkernagel et

JPET Fast Forward. Published on May 16, 2011 as DOI: 10.1124/jpet.111.180521
This article has not been copyedited and formatted. The final version may differ from this version.

al., 2007). Therefore, HIF-1α might participate in the inflammatory response that accompanies APAP-induced liver injury.

In addition to the many factors mentioned above that associate APAP-induced liver injury with hypoxia signaling, HIF-1α can contribute directly to cell death of hepatocytes by upregulation of cell death genes. Nonetheless, it is currently unknown if HIF-1α is involved causally in APAP-induced liver injury. To test the hypothesis that HIF-1α contributes to the pathogenesis of APAP-induced liver injury, conditional HIF-1α-deficient animals were generated and the role of HIF-1α in APAP-induced hepatotoxicity, disruption of hemostasis, and inflammation was evaluated.

METHODS

Materials

Unless otherwise stated, all reagents were purchased from Sigma Chemical Company (St. Louis, MO).

Generation of Conditional HIF-1α-Deficient Animals

HIF-1$\alpha^{flox/flox}$ mice (Ryan et al., 1998) were a gift from Randall Johnson (University of California, San Diego), and UBC-Cre-ERT2$^{+/-}$ mice were purchased from Jackson Laboratories (Bar Harbor, ME). The Cre-ERT2 is regulated by the ubiquitin C promoter and is expressed in virtually all cell types. Cre-ERT2 is a fusion protein composed of Cre recombinase and a mutated estrogen receptor that is selectively activated and targeted to the nucleus by (Z)-1-(p-Dimethylaminoethoxyphenyl)-1,2-diphenyl-1-butene, *trans*-2-[4-(1,2-Diphenyl-1-butenyl)phenoxy]-*N*,*N*-dimethylethylamine [Tamoxifen (TAM)] but not estrogen (Ruzankina et al., 2007). C57Bl/6 HIF-1α$^{flox/flox}$ and UBC-Cre-ERT2$^{+/-}$ transgenic mice were mated to generate UBC-Cre-ERT2$^{+/-}$/HIF-1α$^{flox/flox}$ mice capable of conditional recombination in the floxed HIF-1α gene when treated with TAM. Male UBC-Cre-ERT2$^{+/-}$/HIF-1α$^{flox/flox}$ mice (4-5 weeks old) were treated once per day for 5 days with 200 μg/g body weight TAM in corn oil (OIL) vehicle by oral gavage (Ruzankina et al., 2007). TAM-treated UBC-Cre-ERT2$^{+/-}$/HIF-1α $^{flox/flox}$ mice were HIF-1α deficient (denoted as HIF-1$\alpha^{\Delta/\Delta}$) and OIL-treated animals were HIF-1α sufficient (denoted as HIF-1$\alpha^{+fl/+fl}$) (Fig 1A). UBC-Cre-ERT2$^{-/-}$/HIF-1α$^{flox/flox}$ littermate controls were treated with OIL or TAM to evaluate potential effects of TAM on APAP metabolism. Animals kept in a 12-hour light/dark cycle were fed a standard Rodent chow/Tek 8640 (Harlan Teklad; Madison, WI) and allowed access to water *ad libitum*. All procedures were performed according to the guidelines of the American Association for Laboratory Animal Science and the University Laboratory Animal Research Unit at Michigan State University.

Experimental Protocol

Eleven or twenty-one days after OIL or TAM administration, mice were fasted overnight then given 400 mg/kg APAP or saline (SAL) vehicle via intraperitoneal (i.p.) injection, and food was returned. Mice were anesthetized 2, 6 or 24 hours after APAP with sodium pentobarbital (50 mg/kg, i.p.), and blood was collected from the vena cava into a syringe containing sodium citrate (final concentration 0.76%) for preparation of plasma. The left lateral liver lobe was fixed in 10% formalin and paraffin-blocked for evaluation of histopathology. The left medial lobe was snap frozen in liquid nitrogen for protein, DNA and RNA analysis. The right medial lobe was embedded in Tissue-Tek O.C.T. compound and frozen in liquid nitrogen-cooled isopentane for immunohistochemical analyses.

Genotyping and Real-time PCR

Genotyping of mice was performed for the Cre transgene, HIF-1α, and HIF-1α$^{flox/flox}$ using previously published primer sequences (Saini et al., 2008) (Table 1). Genomic DNA was extracted from tail clippings using the Direct PCR extraction system (Viagen Biotech, Los Angeles, CA) and was used to quantify the Cre transgene. Genotyping of livers from HIF-1α$^{+fl/+fl}$ and HIF-1α$^{\Delta/\Delta}$ mice was performed to determine the recombination efficiency. Genomic DNA was extracted using the Extract-N-Amp system (Sigma Aldrich, St. Louis, MO) per the manufacturer's instructions. PCR conditions were standardized for all alleles: denaturation at 94 °C for 3 min; 38 cycles of denaturation at 94 °C for 45 s, annealing at 60 °C for 45 s, and polymerization at 72 °C for 60 s followed by a 7-min extension at 72 °C.

Gene Expression Analysis

Liver tissue (50 mg) was homogenized in 1 mL of TRI reagent (Sigma Aldrich, St. Louis, MO) using a Precellys 24 Tissue Homogenizer (Cayman Chemicals, Ann Arbor, MI), and RNA was extracted. Total RNA was quantified spectrophotometrically using the NanoDrop 2000 (Thermo Fisher Scientific, Louisville, CO). Total RNA (1 µg) was reverse-transcribed using iScript cDNA synthesis kit (Bio-Rad, Hercules, CA). The expression level of PAI-1, BNIP3 and HIF-1α was analyzed by qRT-PCR using SYBR green (Applied Biosystems, Foster City, CA). Copy number was determined by comparison with

JPET Fast Forward. Published on May 16, 2011 as DOI: 10.1124/jpet.111.180521
This article has not been copyedited and formatted. The final version may differ from this version.

standard curves of the respective genes. Expression level was normalized to the hypoxanthine guanine phosphoribosyl transferase (*HPRT*) gene. Gene-specific primers are listed in Table 1.

Assessment of Hepatocellular Injury and Liver GSH Concentration

Hepatocellular injury was estimated from increases in plasma alanine aminotransferase (ALT) activity and from histopathologic evaluation of fixed tissue. ALT activity was determined spectrophotometrically using Infinity ALT Liquid Stable Reagent (Thermo Electron Corp; Louisville, CO). Paraffin sections of liver (5 μm) were stained with hematoxylin-eosin and examined for evidence of hepatocellular necrosis. To measure GSH concentration, frozen liver samples (100 mg) were homogenized in 1 mL cold buffer (0.2 M 2-*N*-morpholino ethanesulfonic acid, 50 mM phosphate, and 1 mM EDTA; pH 6.0). Homogenates were spun at 10,000 x g for 15 minutes then deproteinated with metaphosphoric acid. Total hepatic GSH concentration was determined spectrophotometrically using a commercially available kit (Cayman Chemical Co.; Ann Arbor, MI).

Immunohistochemistry

Liver sections were stained immunohistochemically for HIF-1α as described previously (Saini et al., 2008). Paraffin was removed from formalin-fixed liver sections (5 μm) and endogenous peroxidase activity was quenched with 6% H_2O_2. Sections were probed with HIF-1α antibody (1:500 dilution, NB100-479, Novus Biologicals; Littleton, CO), which was visualized with Rabbit Vector Elite ABC kit (Vector Laboratories; Burlingame, CA), and sections were counterstained with Nuclear Fast Red. The terminal deoxynucleotidyl transferase-mediated dUTP nick-end labeling (TUNEL) assay was used to analyze DNA fragmentation. Liver sections were stained with the In Situ Cell Death Detection Kit, AP (Roche Diagnostics, Indianapolis, IN) per the manufacturer's instructions. Hepatic fibrin staining was performed as described previously (Copple et al., 2002). Dakocytomation rabbit anti-human/mouse fibrinogen (Dako North America; Carpinteria, CA) was the primary antibody, and a donkey anti-rabbit IgG conjugated to AlexaFluor 488 (Molecular Probes/Invitrogen; Carlsbad, CA) was used as the

secondary antibody. Fibrin images were obtained with an Olympus IX71 inverted fluorescent microscope (Olympus, USA), and positive staining was quantified using Image J software (NIH; Bethesda, MD). Background staining in livers from SAL-treated mice was set as the threshold, and the percentage of pixels above threshold is presented. PMNs were stained as previously described (Maddox et al., 2010), and PMN accumulation was quantified by counting the average number of PMNs in 20 randomly selected high-power fields (400x).

Detection of Bax

Frozen liver sections (5 μm) were fixed in 4% paraformaldehyde for 30 minutes at room temperature. Fixed sections were washed 3 x 7 mins in phosphate buffered saline (PBS) and blocked in 10% donkey serum + 0.1% Triton X-100 (blocking buffer; BB) for 1 hour. Sections were incubated overnight at 4˚C with the following primary antibodies [and their dilutions]: rabbit anti-Bax [1:200] (Cell Signaling Technology, Beverly, MA) and goat anti-cytochrome c oxidase subunit IV (Cox IV) [1:100] (Santa Cruz Biotechnology, Santa Cruz, CA) diluted in BB. After incubation, sections were washed 3 x 7 mins in PBS, blocked in BB for 1 hour, and washed 3 x 7 mins again. Sections were incubated with donkey anti-rabbit Alexa Fluor 568 [1:1000] and donkey anti-goat Alexa Fluor 488 [1:1000] (Invitrogen, Carlsbad, CA) in BB, washed, then mounted with VectaShield Mounting Medium with DAPI (Vector Labs, Burlingame, CA). Slides were stored at -20˚C prior to imaging.

Fluorescent slides were viewed with the Olympus FluoView 1000 confocal laser scanning microscope. Images were collected with Olympus FluoView 1000 software, version 2.0. Alexa Fluor 568 was detected with a 543 nm HeNeG laser with a BA 560-620 emission filter, and Alexa Fluor 488 was detected with a 488 nm Ar laser with a BA 505-525 emission filter. Images were scanned with sequential scan setting for the two lasers. A 60-X oil Plan/APO objective (NA 1.42) was used to acquire images. Five fields of view from each liver section were selected at random. Colocalization of

Bax and Cox IV pixels was analyzed with Image J software (NIH, Bethesda, MD), and data are represented as the percentage of colocalized pixels in an image area.

Evaluation of Plasma and Intrahepatic Cytokine Concentrations

The plasma concentration of active PAI-1 was measured with a commercially available ELISA kit (Molecular Innovations; Novi, MI), following the manufacturer's instructions. The plasma concentrations of IFNγ,IL-1β, IL-2, IL-4, IL-6, IL-10, IL-12 (p70), keratinocyte chemoattractant (KC), macrophage inflammatory protein (MIP)-1α, regulated upon activation normal T cell expressed and secreted (RANTES), TNF-α, and VEGF were measured with a custom Milliplex MAP kit for mouse cytokines (Millipore Corporation; Billerica, MA) using the Bio-Plex 200 System (Bio-Rad Laboratories, Hercules, CA). For determination of hepatic cytokine concentrations, livers were homogenized in 0.1% Triton X-100 in PBS containing Halt Protease and Phosphatase inhibitors (Thermo Fisher Scientific, Louisville, CO), and proteins were quantified by the BCA Assay. Concentrations of KC and RANTES were determined by ELISA (R&D Systems, Minneapolis, MN) and normalized to protein concentrations of the samples.

Statistical analyses

All data are represented as mean ± SEM. Data which were not normally distributed were transformed via Box-cox power transformation. Two or three-way analysis of variance (ANOVA) was used as appropriate, and multiple comparisons were evaluated statistically with appropriate post-hoc tests. $P < 0.05$ was the criterion for significance.

JPET Fast Forward. Published on May 16, 2011 as DOI: 10.1124/jpet.111.180521
This article has not been copyedited and formatted. The final version may differ from this version.

RESULTS

Effect of conditional deletion of HIF-1α gene on liver HIF-1α expression

Conditional HIF-1α knockout mice were generated by mating HIF-1α$^{flox/flox}$ mice (Ryan et al., 1998) with transgenic mice that express the Cre-recombinase transgene (Ruzankina et al., 2007)under the control of the ubiquitin C promoter, and the HIF-1α gene was inactivated upon TAM treatment (Fig 1A). Mice treated with TAM (HIF-1α$^{\Delta/\Delta}$ mice) displayed no obvious phenotypic differences compared to control animals. There was significantly less expression of HIF-1α mRNA in HIF-1α$^{\Delta/\Delta}$ mice compared to HIF-1α$^{+fl/+fl}$ controls (Fig. 1B), demonstrating effective HIF-1α deletion. At 24h, APAP overdose increased expression of HIF-1α mRNA at 24h by 437-fold in HIF-1α$^{+fl/+fl}$. In HIF-1α$^{\Delta/\Delta}$ mice, there was a modest increase in HIF-1α mRNA expression (by 26-fold) at 24h. Expression of HIF-1α protein in livers was evaluated immunohistochemically 2h after SAL or APAP treatment. SAL-treated HIF-1α$^{+fl/+fl}$ mice had minimal staining, whereas HIF-1α staining was not observed in HIF-1α$^{\Delta/\Delta}$ mice (Fig 1C). APAP overdose increased hepatocellular HIF-1α staining in HIF-1α$^{+fl/+fl}$ mice; the staining appeared to be cytoplasmic in most cells, with some nuclear staining. This supports previous evidence that APAP overdose caused HIF-1α accumulation in mouse liver (James et al., 2006; Chaudhuri et al., 2011). There was markedly less HIF-1α staining in HIF-1α$^{\Delta/\Delta}$ mice treated with APAP, confirming successful deletion of HIF-1α.

HIF-1α inactivation protects from early APAP hepatotoxicity

To determine whether TAM treatment could affect APAP hepatotoxicity, UBC-Cre-ERT2$^{(-/-)}$/ HIF-1α$^{flox/flox}$ mice, which do not express a functional Cre recombinase and cannot remove HIF-1α, were treated with OIL or TAM for 5 days, and 3 weeks later were treated with saline (SAL) or 400 mg/kg APAP. Both OIL- and TAM-treated mice developed severe liver injury 6h after treatment, indicating that TAM alone did not affect APAP hepatotoxicity (Fig 2). In contrast, when UBC-Cre-ERT2$^{+/-}$/HIF-1α$^{flox/flox}$ mice, which are capable of TAM-induced Cre recombination, underwent the same treatments, OIL-treated UBC-

JPET Fast Forward. Published on May 16, 2011 as DOI: 10.1124/jpet.111.180521
This article has not been copyedited and formatted. The final version may differ from this version.

Cre-ERT2$^{+/-}$/HIF-1α$^{flox/flox}$ mice (HIF-1α-sufficient) developed severe liver injury 6h after treatment, but injury was essentially absent in TAM-treated UBC-Cre-ERT2$^{+/-}$/HIF-1α $^{flox/flox}$ mice (HIF-1α-deficient) (Fig. 2), indicating that the acute liver injury dependedon HIF-1α signaling. All subsequent experiments were performed in UBC-Cre-ERT2$^{+/-}$/HIF-1α$^{flox/flox}$ mice.

Time course of APAP hepatotoxicity

HIF-1α$^{+fl/+fl}$ mice treated with APAP had significantly greater plasma ALT activity at 2h compared to SAL-treated animals, which developed into severe liver injury by 6h and continued to increase through 24h (Fig. 3A). APAP treated, HIF-1α$^{\Delta/\Delta}$ mice had complete attenuation of liver injury at 2h and 6h, however plasma ALT activity was the same as in HIF-1α$^{+fl/+fl}$ mice at 24h. Histological analysis confirmed centrilobular hepatocellular necrosis in HIF-1α$^{+fl/+fl}$ mice at 6h and 24h after APAP overdose and that HIF-1α$^{\Delta/\Delta}$ mice had no lesions at 6h but significant lesions at 24h (Fig 3B). Hepatic GSH depletion was used as an indication of APAP bioactivation. HIF-1α$^{+fl/+fl}$ and HIF-1α$^{\Delta/\Delta}$ mice treated with SAL had 4.4 ± 0.5 and 5.3 ± 0.6 μmol glutathione/g liver, respectively. After APAP administration, glutathione concentration was reduced in HIF-1α$^{+fl/+fl}$ and HIF-1α$^{\Delta/\Delta}$ mice to 0.4 ± 0.02 and 1.52 ± 1.1 μmol/g liver, respectively; these values were not significantly different from one another.

Expression of cell death proteins

The contribution of HIF-1α to production of cell death proteins in APAP overdose was evaluated. APAP overdose did not affect the expression of BNIP3 mRNA in liver (Table 2), nor did it alter hepatic expression of BNIP3 protein (data not shown). Bax is a proapoptotic protein that translocates to the mitochondria upon activation and contributes to APAP-induced hepatocellular necrosis (Bajt et al., 2008a). In the livers of HIF-1α$^{+fl/+fl}$ mice, APAP overdose increased the colocalization of Bax with Cox IV, a mitochondrial marker (Fig 4). In contrast this effect was not observed in APAP-treated HIF-1α$^{\Delta/\Delta}$ mice. APAP overdose caused DNA fragmentation in centrilobular hepatocytes in HIF-1α$^{+fl/+fl}$ mice at 6 and 24h; this effect was attenuated upon HIF-1α deletion (Fig. 5).

HIF-1α deletion attenuates coagulation system activation

Thrombin-antithrombin (TAT) concentration reflects the activation of thrombin in plasma. In HIF-1α$^{+fl/+fl}$ mice, plasma TAT concentration was significantly increased by APAP overdose 2, 6 and 24h after treatment, although it was somewhat less at 24h. In HIF-1α$^{\Delta/\Delta}$ mice, plasma TAT was elevated 2h after APAP, returned to baseline at 6h, then increased significantly by 24h to a concentration greater than the value in HIF-1α$^{+fl/+fl}$ mice (Fig. 6A). A consequence of thrombin activation in liver is deposition of fibrin, which was assessed by immunohistochemical staining. In HIF-1α$^{+fl/+fl}$ mice, fibrin deposition was detected at 6h after overdose and increased significantly by 24h. In contrast, there was no fibrin deposition in HIF-1α$^{\Delta/\Delta}$ mice detected until 24h after APAP (Fig. 6B). In HIF-1α$^{+fl/+fl}$ mice, fibrin deposition at 6h appeared to be centrilobular and sinusoidal after APAP overdose (Fig. 6C).

The fibrinolytic system consists of plasminogen and the plasminogen activators (PAs), tPA and uPA, which cleave plasminogen to plasmin to dissolve fibrin clots. PAI-1 is the endogenous inhibitor of PAs, and elevation of active PAI-1 in plasma suggests inhibition of fibrinolysis. Hepatic PAI-1 mRNA was measured 2, 6, and 24h after treatment. In SAL-treated mice, basal PAI-1 mRNA expression was small (Table 3). In HIF-1α$^{+fl/+fl}$ mice treated with APAP, hepatic PAI-1 mRNA was elevated by more than 10-fold as early as 2h after APAP and remained so through 24h. In HIF-1α$^{\Delta/\Delta}$ mice, PAI-1 mRNA increased to the same level as HIF-1α$^{+fl/+fl}$ mice 2h after APAP, then decreased to baseline at 6h only to increase again by 24h. The circulating concentration of active PAI-1 was also evaluated at 6h and 24h. In HIF-1α$^{+fl/+fl}$ mice, APAP overdose increased the appearance of active PAI-1 in plasma at 6h, and PAI-1 concentration increased further by 24h (Fig. 7). This increase in PAI-1 was attenuated in HIF-1α$^{\Delta/\Delta}$ mice at 6h but was similar to that seen in HIF-1α$^{+fl/+fl}$ mice by 24h.

The role of HIF-1α in the inflammatory response to APAP

Plasma concentrations of cytokines were measured 6h after APAP exposure. Neither HIF-1α deletion nor APAP overdose affected the plasma concentrations of IL-1β, IL-2, IL-4, TNFα, MIP-1α or VEGF at

these times (Table 4). APAP overdose increased plasma concentrations of IL-6, RANTES, and KC in HIF-1α$^{+fl/+fl}$ mice, and these increases were significantly attenuated upon HIF-1α deletion (Table 4). Plasma concentrations of IL-6, KC and RANTES were evaluated 24h after APAP treatment. APAP overdose increased IL-6 (Fig. 8A) and KC (Fig 8B) in both HIF-1α$^{+fl/+fl}$ and HIF-1α$^{\Delta/\Delta}$ mice at 24h, however there were no changes in RANTES (data not shown). Intrahepatic concentrations of KC and RANTES were also determined. Hepatic RANTES was not altered by APAP (Fig. 8C), but hepatic KC was significantly increased at 6 and 24h after APAP overdose in HIF-1α$^{+fl/+fl}$ mice, and by 24h in HIF-1α$^{\Delta/\Delta}$ mice (Fig. 8D). KC is a chemokine important for PMN infiltration, so hepatic PMNs were quantified. There were significantly fewer PMNs in the livers of HIF-1α$^{\Delta/\Delta}$ mice 6 and 24 hours after APAP administration compared to HIF-1α$^{+fl/+fl}$ mice (Fig. 9).

DISCUSSION

HIF-1α deletion protected mice from early APAP-induced liver injury, but it did not prevent the development of severe liver injury 24h after overdose (Fig. 3). The protection from toxicity at 2 and 6h was not due to decreased bioactivation, since the depletion of GSH was similar in HIF-1α$^{+fl/+fl}$ and HIF-1α$^{\Delta/\Delta}$ mice. These data suggest that HIF-1α has dual roles in the pathogenesis of APAP-induced liver injury. HIF-1α appears to have a damaging role in early progression of injury, possibly through its contribution to insertion of Bax into the mitochondria (Fig. 4), hemostasis (Fig. 6 and 7), and/or the inflammatory response (Table 4, Fig. 8 and 9). The loss of protection at 24h suggests that HIF-1α has a protective role at later times, or that its absence delays the onset of liver injury. The former suggestion is consistent with a recently published report indicating that hepatocytes exposed to moderate hypoxia were protected from APAP-induced cell death (Yan et al., 2010). The protective effect of hypoxia was attributed to hypoxic preconditioning, because HIF-1α can induce the transcription of protective factors, such as heme oxygenase-1 or erythropoietin (Bernhardt et al., 2007). Furthermore, Kato *et al* (2011) found that the HIF-1α-regulated gene VEGF is important in liver repair from APAP overdose.

APAP overdose increased hepatic HIF-1α protein at 2h in HIF-1α$^{+fl/+fl}$ mice (Fig. 1C), an effect that was attenuated in HIF-1α$^{\Delta/\Delta}$ mice. This is consistent with recently published reports that APAP overdose caused nuclear accumulation of HIF-1α in liver extracts and isolated mouse hepatocytes 1h after treatment, an effect which was maintained through 12h (James et al., 2006; Chaudhuri et al., 2011). HIF-1α accumulation occurred prior to the development of hypoxia in the liver (Chaudhuri et al., 2011), suggesting that the initial mechanism by which HIF-1α is stabilized is independent of hypoxia. However, the coagulation system is activated and fibrin deposits in the liver beginning 2h after administration of APAP (Ganey et al., 2007) and tissue hypoxia becomes apparent between 2 and 4h (Chaudhuri et al., 2011); accordingly coagulation-dependent hypoxia could contribute to prolonged stabilization of HIF-1α during the progression of liver injury.

JPET Fast Forward. Published on May 16, 2011 as DOI: 10.1124/jpet.111.180521
This article has not been copyedited and formatted. The final version may differ from this version.

APAP overdose caused HIF-1α-dependent translocation of Bax to the mitochondrial membrane (Fig.4). APAP overdose causes JNK-dependent Bax insertion into the mitochondrial membrane beginning 1h after treatment (Saito et al., 2010), and $Bax^{-/-}$ mice were protected from APAP hepatotoxicity at 6h, but not 12h (Bajt et al., 2008a). The authors hypothesized that Bax contributes to early MPT formation and release of mitochondrial intermembrane proteins that initiate DNA fragmentation and hepatocellular necrosis, but that continuous oxidative stress supplants this mechanism to cause cell damage at later times. Our observation that HIF-$1\alpha^{\Delta/\Delta}$ mice had reduced Bax translocation (Fig. 4) at 6h after APAP is consistent with this hypothesis. Additionally, APAP-induced DNA fragmentation was attenuated in HIF-$1\alpha^{\Delta/\Delta}$ mice compared to HIF-$1\alpha^{+fl/+fl}$ animals (Fig 5). These data suggest that HIF-1α is necessary for early Bax translocation and DNA fragmentation, however other APAP-induced signaling overcomes this protection by 24h.

In addition to its role in cell death signaling, HIF-1α might contribute to APAP-induced liver injury by modulating the hemostatic system. APAP overdose activates the coagulation system and results in sinusoidal fibrin deposition in mice (Ganey et al., 2007), and it is associated with alterations in plasma hemostatic factors in humans (James et al., 2002). Furthermore, reduction in coagulation attenuated liver injury 6h, but not 24h after APAP overdose in mice (Ganey et al., 2007), similar to our current finding in HIF-$1\alpha^{\Delta/\Delta}$ mice (Fig. 3). In the absence of HIF-1α expression, there was significant attenuation of thrombin generation (Fig. 6A) and fibrin deposition (Fig. 6B) at 6h. By 24h, thrombin generation in HIF-$1\alpha^{\Delta/\Delta}$ mice had exceeded that seen HIF-$1\alpha^{+fl/+fl}$ mice at the same time, and there was significant sinusoidal fibrin (Fig. 6B). This raises the possibility that the protection afforded by HIF-1α deletion is mediated by its ability to delay thrombin generation and fibrin deposition, thereby delaying the development of liver injury. However, it is also possible that in the absence of liver injury in HIF-$1\alpha^{\Delta/\Delta}$ mice at 2 and 6h, there is not a stimulus for activation of thrombin.

HIF-1α also plays a role in fibrinolysis through regulation of PAI-1 expression (Copple et al., 2009). In the present study, hepatic PAI-1 mRNA and plasma protein were elevated at all times measured in

JPET Fast Forward. Published on May 16, 2011 as DOI: 10.1124/jpet.111.180521
This article has not been copyedited and formatted. The final version may differ from this version.

APAP-treated HIF-1α$^{+fl/+fl}$ mice (Table 3), consistent with previous findings (Ganey et al., 2007; Bajt et al., 2008b). In contrast, in HIF-1α$^{\Delta/\Delta}$ mice PAI-1 mRNA was elevated at 2h, returned to baseline by 6h, then increased to the same level as HIF-1α$^{+fl/+fl}$ mice by 24h (Table 3). The appearance of active PAI-1 in the plasma followed a similar pattern (Fig. 7). This results raises the possibility that during APAP overdose, PAI-1 expression is a consequence of hepatocellular death and hemostasis, rather than due to a direct regulatory role by HIF-1α; indeed other transcription factors such as egr-1 and HIF-2α contribute to PAI-1 expression (Copple et al., 2009). PAI-1$^{-/-}$ mice had enhanced liver necrosis and increased mortality after administration of 200 mg/kg APAP compared to control animals, suggesting a protective role for PAI-1; the enhanced liver injury in PAI-1 $^{-/-}$ mice was associated with decreased expression of proliferating cell nuclear antigen (PCNA) and was therefore attributed to delayed tissue repair (Bajt et al., 2008b).

Appropriate tissue repair is necessary for recovery from liver injury (Mehendale, 2005), and the HIF-1α-regulated gene VEGF has recently been identified as an important mediator of tissue repair after APAP hepatotoxicity (Donahower et al., 2006; Kato et al., 2011). We found no increase in plasma VEGF at 6h (Table 4), which is in contrast with previously published reports in which hepatic VEGF protein was increased starting 8h after APAP overdose (Donahower et al., 2006; Kato et al., 2011). VEGF is produced by hepatocytes and acts locally on sinusoidal endothelial cells, therefore it might not have reached detectable concentrations in plasma. VEGF plays an important role in hepatocyte regeneration and restoration of liver microvasculature, through activation of repair pathways (Donahower et al., 2006) and angiogenesis (Kato et al., 2011). Since VEGF is regulated by HIF-1α, it is possible that the progression of liver injury between 6 and 24 hr in HIF-1α$^{\Delta/\Delta}$ mice occurs because of loss of regeneration and other repair mechanism that are initiated by VEGF.

APAP overdose is associated with increases in inflammatory cytokines, and the role of HIF-1α in the production of cytokines is well documented in other conditions. Mice with HIF-1α-deficient monocytes produced less TNFα, IL-6, IL-12, IL-1α and IL-1β in response to LPS compared to wild type animals

(Peyssonnaux et al., 2007). In human patients, large plasma concentrations of IL-6, IL-8 and MCP-1 correlated with the severity of liver injury due to APAP overdose (James et al., 2005).. Furthermore, APAP overdose increased plasma concentrations of IL-1β, IL-6, KC, MCP-1, MIP-2 and TNFα in mice (Ishida et al., 2002; Ishida et al., 2004). In our study, APAP overdose caused an increase in plasma concentrations of IL-6, KC, and RANTES at 6h in HIF-1α$^{+fl/+fl}$ mice, which was attenuated by deletion of HIF-1α (Table 4). Additionally, APAP overdose increased hepatic concentration of KC 6 and 24h after treatment in HIF-1α$^{+fl/+fl}$ mice, and 24h after treatment in HIF-1α$^{\Delta/\Delta}$ mice (Fig. 7). KC is a chemokine important for the recruitment of PMNs to the liver. HIF-1α$^{\Delta/\Delta}$ mice had smaller plasma concentrations of KC and RANTES at 6h (Table 4), which was associated with fewer hepatic PMNs 6 and 24h after APAP compared to HIF-1α$^{+fl/+fl}$ mice (Fig. 6).

The role of PMNs in APAP-induced liver injury remains controversial (Jaeschke, 2008). There is evidence that PMNs promote liver injury (Liu et al., 2006; Jaeschke, 2008) in APAP overdose, however more recent evidence suggests that they accompany the sterile inflammatory response but do not contribute to injury (Jaeschke, 2008; Williams et al., 2010). PMNs are necessary for the phagocytosis of necrotic hepatocytes in APAP hepatotoxicity (Lawson et al., 2000). HIF-1α-deficient monocytes have reduced phagocytic capacity and reduced release of antimicrobial proteins and granule proteases such as elastase and cathepsin G (Cramer et al., 2003; Zinkernagel et al., 2007), raising the possibility that HIF-1α$^{\Delta/\Delta}$ mice might have reduced ability to phagocytose necrotic hepatocytes and thus reduced tissue repair capacity. This might explain why hepatocellular injury appears to return by 24h.

In summary, deletion of HIF-1α protects mice from early progression of APAP-induced liver injury, but does not afford lasting protection. At early times, HIF-1α regulates Bax translocation to the mitochondria and consequent DNA fragmentation that results in hepatocellular necrosis. It also contributes to regulation of the coagulation and fibrinolytic systems, as well as to the production of inflammatory mediators that can influence the pathogenesis of APAP-induced liver injury. At later times, HIF-1α deletion does not protect from severe liver injury, possibly through regulation of factors

JPET Fast Forward. Published on May 16, 2011 as DOI: 10.1124/jpet.111.180521
This article has not been copyedited and formatted. The final version may differ from this version.

that support tissue repair and regeneration, such as PMN infiltration, VEGF and PAI-1. Our results suggest that HIF-1α has dual roles in APAP-induced liver injury, promoting damage early and conferring protection later during the pathogenesis.

ACKNOWLEDGMENTS

The authors would like to thank Karen Kassel, Nicole Crisp and Allen Macdonald for technical assistance.

AUTHORSHIP CONTRIBUTIONS

Participated in research design: Sparkenbaugh, Saini, LaPres, Copple, Luyendyk, Maddox, Ganey, Roth

Conducted experiments: Sparkenbaugh, Luyendyk, Maddox

Contributed new reagents or analytical tools: LaPres, Saini, Greenwood

Performed data analysis: Sparkenbaugh

Wrote or contributed to the writing of the manuscript: Sparkenbaugh, LaPres, Copple, Luyendyk, Ganey, Roth

REFERENCES

Bajt ML, Farhood A, Lemasters JJ and Jaeschke H (2008a) Mitochondrial bax translocation accelerates DNA fragmentation and cell necrosis in a murine model of acetaminophen hepatotoxicity. *J Pharmacol Exp Ther* **324**:8-14.

Bajt ML, Yan H-M, Farhood A and Jaeschke H (2008b) Plasminogen Activator Inhibitor-1 Limits Liver Injury and Facilitates Regeneration after Acetaminophen Overdose. *Toxicol Sci* **104**:419-427.

Bernhardt WM, Warnecke C, Willam C, Tanaka T, Wiesener MS and Eckardt KU (2007) Organ protection by hypoxia and hypoxia-inducible factors. *Methods Enzymol* **435**:221-245.

Chaudhuri S, McCullough SS, Hennings L, Letzig L, Simpson PM, Hinson JA and James LP (2011) Acetaminophen hepatotoxicity and HIF-1alpha induction in mice occur without hypoxia. *Toxicol Appl Pharmacol*.[in press]

Copple BL, Banes A, Ganey PE and Roth RA (2002) Endothelial cell injury and fibrin deposition in rat liver after monocrotaline exposure. *Toxicol Sci* **65**:309-318.

Copple BL, Bustamante J, Welch T, Kim N and Moon J (2009) Hypoxia-inducible factor-dependent production of profibrotic mediators by hypoxic hepatocytes. *Liver Int* **29(7)**:1010-1021.

Cover C, Liu J, Farhood A, Malle E, Waalkes MP, Bajt ML and Jaeschke H (2006) Pathophysiological role of the acute inflammatory response during acetaminophen hepatotoxicity. *Toxicol Appl Pharmacol* **216**:98-107.

Cramer T, Yamanishi Y, Clausen B, Forster I, Pawlinski R, Mackman N, Haase V, Jaenisch R, Corr M, Nizet V, Firestein G, Gerber H and Ferrar N (2003) HIF-1alpha Is Essential for Myeloid Cell-Mediated Inflammation. *Cell* **112**:645-657.

Cursio R, Miele C, Filippa N, Van OE and Gugenheim J (2008) Liver HIF-1alpha induction precedes apoptosis following normothermic ischemia-reperfusion in rats. *Transplant Proc* **40**:2042-2045.

Donahower B, McCullough SS, Kurten R, Lamps LW, Simpson P, Hinson JA and James LP (2006) Vascular endothelial growth factor and hepatocyte regeneration in acetaminophen toxicity. *AmJPhysiol Gastrointest Liver Physiol* **291**:G102-G109.

Ganey P, Luyendyk J, Newport S, Eagle T, Maddox J, Mackman N and Roth R (2007) Role of the coagulation system in acetaminophen-induced hepatotoxicity in mice. *Hepatology* **46(4)**:1177-1186.

Gorlach A, Diebold I, Schini-Kerth VB, Berchner-Pfannschmidt U, Roth U, Brandes RP, Kietzmann T and Busse R (2001) Thrombin activates the hypoxia-inducible factor-1 signaling pathway in vascular smooth muscle cells: Role of the p22(phox)-containing NADPH oxidase. *Circ Res* **89**:47-54.

Haddad J and Harb H (2005) Cytokines and the regulation of hypoxia-inducible factor (HIF)-1α. *Int Immunopharmacol* **5:**461-483.

Ishida Y, Kondo T, Ohshima T, Fujiwara H, Iwakura Y and Mukaida N (2002) A Pivotal Involvement of IFN-gamma in the Pathogenesis of Acetaminophen-induced Acute Liver Injury. *FASEB J* **16(10)**:1227-1236.

Ishida Y, Kondo T, Tsuneyama K, Lu P, Takayasu T and Mukaida N (2004) The pathogenic roles of tumor necrosis factor receptor p55 in acetaminophen-induced liver injury in mice. *J Leuk Biol* **75**:59-67

Jaeschke H (2008) Innate Immunity and Acetaminophen -Induced Liver Injury: Why So Many Controversies? *Hepatology* **48**:699-701.

James LP, Simpson PM, Farrar HC, Kearns GL, Wasserman GS, Blumer JL, Reed MD, Sullivan JE and Hinson JA (2005) Cytokines and Toxicity in Acetaminophen Overdose. *J Clin Pharmacol* **45**:1165-1171.

James LP, Wells E, Beard RH and Farrar HC (2002) Predictors of outcome after acetaminophen poisoning in children and adolescents. *J of Pediatr* **140**:522-526.

James LP, Donahower B, Burke A, McCullough S and Hinson JA (2006) Induction of the nuclear factor HIF-1alpha in acetaminophen toxicity: Evidence for oxidative stress. *Biochem Biophys Res Comm* **343**:171-176.

James LP, McCullough S, Lamps LW and Hinson J (2003) Effect of N-Acetylcysteine of Acetaminophen Toxicity in Mice: Relationship to Reactive Nitrogen and Cytokine Formation. *Toxicol Sci* **75**:458-467.

Jollow DJ, Mitchell JR, Potter WZ, Davis DC, Gillette JR and Brodie BB (1973) Acetaminophen-induced hepatic necrosis. II. Role of covalent binding in vivo. *J Pharmacol Exp Ther* **187**:195-202.

Kato T, Ito Y, Hosono K, Suzuki T, Tamaki H, Minamino T, Kato S, Sakagami H, Shibuya M and Majima M (2011) Vascular endothelial growth factor receptor-1 signaling promotes liver repair through restoration of liver microvasculature after acetaminophen hepatotoxicity. *Toxicol Sci* **120**:218-229.

Kim H, Kim Y, Nam B, Kong H, Kim H, Kim Y, An W and Cheong J (2007) HIF-1α expression in response to lipopolysaccharide mediates induction of hepatic inflammatory cytokine TNFα. *Exp Cell Res* **313**:1866-1876

Klimova TA and Chandel N (2008) Mitochondrial Complex III regulates hypoxia activation of HIF. *Cell Death Differ* **15**:660-666.

Lawson JA, Farhood A, Hopper RD, Bajt ML and Jaeschke H (2000) The Hepatic Inflammatory Response after Acetaminophen Overdose: Role of Neutrophils. *Toxicol Sci* **54**:509-516.

Lee K, Roth R and LaPres J (2007) Hypoxia, drug therapy and toxicity. *Pharmacol Ther* **113**:229-246.

Lee WM (2007) Acetaminophen toxicity: changing perceptions on a social/medical issue. *Hepatology* **46**:966-970.

Li L, Chen SH, Zhang Y, Yu CH, Li SD and Li YM (2006) Is the hypoxia-inducible factor-1 alpha mRNA expression activated by ethanol-induced injury, the mechanism underlying alcoholic liver disease? *Hepatobiliary Pancreat Dis Int* **5**:560-563.

Liu Z-X, Han D, Gunawan B and Kaplowitz N (2006) Neutrophil Depletion Protects Against Murine Acetaminophen Hepatotoxicity. *Hepatology* **43**:1220-1230.

Maddox JF, Amuzie CJ, Li M, Newport SW, Sparkenbaugh E, Cuff CF, Pestka JJ, Cantor GH, Roth RA and Ganey PE (2010) Bacterial- and viral-induced inflammation increases sensitivity to acetaminophen hepatotoxicity. *J Toxicol Environ Health A* **73**:58-73.

Masubuchi Y, Bourdi M, Reilly T, Graf M, George JW and Pohl LR (2003). Role of interleukin-6 in hepatic heat shock protein expression and protection against acetaminophen-induced liver disease. *Biochem Biophys Res Comm* **304**:207-212.

Mehendale HM (2005) Tissue repair: an important determinant of final outcome of toxicant-induced injury. *Toxicol Pathol* **33**:41-51.

Murdoch C, Muthana M and Lewis C (2005) Hypoxia Regulates Macrophage Functions in Inflammation. *J Immunol* **175**:6257-6263.

Peyssonnaux C, Cejudo-Martin P, Doedens A, Zinkernagel A, Johnson R and Nizet V (2007) Cutting Edge: Essential Role of Hypoxia Inducible Factor 1a in Development of Lipopolysaccharide-Induced Sepsis. *J Immunol* **178**:7516-7519.

Peyssonnaux C, Datta V, Cramer T, Doedens A, Theodorakis E, Gallo R, Hurtado-Ziola N, Nizet V and Johnson R (2005) HIF-1α expression regulates the bactericidal capacity of phagocytes. *J Clin Invest* **115(7)**:1806-1815.

Ruzankina Y, Pinzon-Guzman C, Asare A, Ong T, Pontano L, Cotsarelis G, Zediak VP, Velez M, Bhandoola A and Brown EJ (2007) Deletion of the developmentally essential gene ATR in adult mice leads to age-related phenotypes and stem cell loss. *Cell Stem Cell* **1**:113-126.

Ryan HE, Lo J and Johnson RS (1998) HIF-1α is required for solid tumor formation and embryonic vascularization. *EMBO J* 17(11), 3005-3015.

Saini Y, Harkema J and LaPres J (2008) HIF-1α is essential for normal intrauterine differentiation of alveolar epithelium and surfactant production in the newborn lung of mice. *J Biol Chem* **283**:33650-33657.

Saito C, Lemasters JJ and Jaeschke H (2010) c-Jun N-terminal kinase modulates oxidant stress and peroxynitrite formation independent of inducible nitric oxide synthase in acetaminophen hepatotoxicity.*Toxicol Appl Pharmacol* **246**:8-17.

Walmsley S, Cadwallader K and Chilvers E (2005a) The role of HIF-1α in myeloid cell inflammation. *TRENDS Immunol* **26(8)**:434-439.

Walmsley S, Print C, Farahi N, Peyssonnaux C, Cramer T, Sobolewski A, Condliffe A, Cowburn A, Johnson N and Chilvers E (2005b) Hypoxia-induced neutrophil survival is mediated by HIF-1α-dependent NF-kB activity. *J Exp Med* **201**:105-115.

Williams CD, Farhood A and Jaeschke H. Role of caspase-1 and interleukin-1β in acetaminophen-induced hepatic inflammation and liver injury. *Toxicol Appl Pharmacol* **247(3)**:169-178.

Yan H-M, Ramachandran A, Bajt ML, Lemasters JJ and Jaeschke H (2010) The Oxygen Tension Modulates Acetaminophen-Induced Mitochondrial Oxidant Stress and Cell Injury in Cultured Hepatocytes. *Toxicol Sci* **117(2)**:525-523.

Zinkernagel A, Johnson RS and Nizet V (2007) Hypoxia inducible factor (HIF) in innate immunity and infection. *J Mol Med* **85**:1339-1346.

FOOTNOTES

A) This research was supported by National Institutes of Health [Grant R01ES004139] and [Grant R01ES12186]. E.M.S. was supported in part by NIEHS training grant T32 ES007255

B) Sparkenbaugh, EM, Saini, Y, LaPres, JJ, Maddox, JF, Ganey, PE, and Roth, RA. (2010) HIF-1α deletion protects mice from acetaminophen hepatotoxicity and reduces activation of the hemostatic system. *The Toxicologist.* The Society of Toxicology Annual Meeting.

C) Reprint requests:
Robert A. Roth, PhD, DABT
221 Food Safety and Toxicology Center
Michigan State University
East Lansing, MI 48824
rothr@msu.edu
Phone: 517-353-9841
Fax: 517-432-2310

JPET Fast Forward. Published on May 16, 2011 as DOI: 10.1124/jpet.111.180521
This article has not been copyedited and formatted. The final version may differ from this version.

LEGENDS FOR FIGURES

Fig 1. Conditional HIF-1α deletion in mice. . Five week old CRE-ERT2$^{(+/-)}$/HIF-1α$^{flox/flox}$ mice were treated with OIL or 200 μg/g TAM for five days to generate HIF-1α$^{+fl/+fl}$ or HIF-1α$^{\Delta/\Delta}$ mice (**A**). 21 days later, mice were treated with 400 mg/kg APAP or SAL intraperitoneally. Liver samples were taken 2 and 6 hours after APAP administration. (**B**) HIF-1α mRNA was measured in liver tissue and is expressed as an average of the ratios of HIF-1α:HPRT copy number normalized to SAL controls. (**C**) Formalin-fixed livers were stained for HIF-1α protein, which appears as dark brown stain. Arrows indicate positive staining.

Fig. 2. Effect of HIF-1α deletion on APAP hepatotoxicity. Five week old CRE-ERT2$^{-/-}$/HIF-1α$^{flox/flox}$ (labeled Cre (-)/HIF-1α$^{fl/fl}$) or CRE-ERT2$^{+/-}$/HIF-1α$^{flox/flox}$ (labeled Cre (+)/HIF-1α$^{fl/fl}$) mice were treated with OIL or 200 μg/g TAM daily for five days. 21 days later, mice were treated with APAP or SAL intraperitoneally. Plasma alanine aminotransferase (ALT) activity was measured 6h after APAP administration. Data represent means ± SEM of n = 3-8 animals per group. *a* Significantly different from SAL-treated mice; *b* Significantly different from OIL-treated mice; *c* Significantly different from HIF-1α$^{+fl/+fl}$ mice.

Fig 3. Time course of APAP-induced liver injury in HIF-1α-deficient mice. HIF-1α$^{+fl/+fl}$ or HIF-1α$^{\Delta/\Delta}$ mice were treated with APAP (400 mg/kg) or SAL, and plasma and liver samples were taken 2h, 6h and 24h after later. (**A**) Liver injury was assessed from plasma ALT activity; data represent means ± SEM of n = 3-8 animals per group. (**B**) Livers were processed for histology and stained with H&E. Sections are shown from mice with ALT values near the median. *a* Significantly different from SAL-treated mice; *b* Significantly different from APAP-treated HIF-1α$^{+fl/+fl}$ mice; *c* Significantly different from same treatment at 2 h.

Fig. 4 Mitochondrial Bax translocation. Mice were treated with SAL or 400 mg/kg APAP, and 6h later liver samples were taken. (**A**) Quantification of Bax: Cox IV colocalization was performed as described

JPET Fast Forward. Published on May 16, 2011 as DOI: 10.1124/jpet.111.180521
This article has not been copyedited and formatted. The final version may differ from this version.

in Methods. (**B**) Representative 60X confocal fluorescent micrographs of frozen liver sections from 2-3 animals per group. There were no significant differences between SAL treated HIF-1α$^{+fl/+fl}$ and HIF-1α$^{\Delta/\Delta}$ mice, so they were combined for statistical purposes. *a* Significantly different from SAL-treated mice.

Fig. 5 DNA fragmentation after APAP treatment. DNA fragmentation was evaluated by the TUNEL assay inHIF-1α$^{+fl/+fl}$ and HIF-1α$^{\Delta/\Delta}$ mice treated with SAL or 400 mg/kg APAP 6 or 24h earlier (200x for all panels).

Fig 6. Effect of HIF-1α deletion on thrombin production and fibrin deposition.SAL or 400 mg/kg APAP was administered to HIF-1α$^{+fl/+fl}$ and HIF-1α$^{\Delta/\Delta}$ mice, and plasma and liver samples were taken 2, 6 and 24h later. (**A**) Plasma TAT dimer was measured as a marker of thrombin generation. Frozen liver samples were stained immunohistochemically for fibrin. (**B**) Quantification of fibrin. (**C**)Representative liver sections from HIF-1α$^{+fl/+fl}$ and HIF-1α$^{\Delta/\Delta}$ mice treated with APAP. *a* Significantly different from SAL-treated mice; *b* Significantly different from APAP-treated HIF-1α$^{+fl/+fl}$ mice.; *c* Significantly different from same group at 2 and 6h.

Fig. 7. Effect of HIF-1α deletion on PAI-1 production. 400 mg/kg APAP or SAL was administered to HIF-1α$^{+fl/+fl}$ and HIF-1α$^{\Delta/\Delta}$ mice, and plasma samples were taken after 2, 6 or 24 h. Active PAI-1 protein was measured in plasma, and data represent means ± SEM of n = 3-8 animals per group. *a* Significantly different from SAL-treated mice; *b* Significantly different from APAP-treated HIF-1α$^{+fl/+fl}$ mice.

Fig. 8. Hepatic and plasma concentration of cytokines. Plasma concentration of IL-6 and KC were measured at 24h, and liver lysates were prepared and the concentrations of KC and RANTES determined 6 and 24h after SAL or APAP. Data represent means ± SEM of n = 3-8 animals per group. (**A**) Plasma IL-6 concentration at 24h. (**B**) Plasma KC concentration at 24h. (**C**) Hepatic RANTES concentration. (**D**) Hepatic KC concentration. *a* Significantly different from SAL-treated mice; *b*

Significantly different from APAP-treated HIF-1α$^{+fl/+fl}$ mice; *c* Significantly different from same treatment at 6h

Fig. 9: Hepatic PMN accumulation after APAP treatment in HIF-1α$^{+fl/+fl}$ and HIF-1α$^{\Delta/\Delta}$ mice. (**A**) PMNs were quantified in 20 randomly selected high-power fields (HPF; 400x). Data represent means ± SEM of n = 3-8 animals per group. *a* Significantly different from SAL; *b* Significantly different from APAP-treated HIF-1α$^{+fl/+fl}$ mice; *c* Significantly different from same group at 6h. (**B**) Representative sections from HIF-1α$^{+fl/+fl}$ and HIF-1α$^{\Delta/\Delta}$ mice.

JPET Fast Forward. Published on May 16, 2011 as DOI: 10.1124/jpet.111.180521
This article has not been copyedited and formatted. The final version may differ from this version.

TABLES

Table 1: Primer sequences

Allele	**Forward (5'-3')**	**Reverse (5'-3')**
BNIP3	TGCAGGCACCTTTATCACTCTGCT	CGCCCGATTTAAGCAGCTTTGGAT
Cre Transgene	TGCCACGACCAAGTGACAGCAATG	AGAGACGGAAATCCATCGCTCG
HIF-1α	CGTGTGAGAAAACTTCTGGATG	CATGTCGCCGTCATCTGTTA
HIF-1α (flox)	TTGGGGATGAAAACATCTGC	CATGTCGCCGTCATCTGTTA
HPRT	AGGAGTCCTGTTGATGTTGCCAGT	GGGACGCAGCAACTGACATTTCTA

JPET Fast Forward. Published on May 16, 2011 as DOI: 10.1124/jpet.111.180521
This article has not been copyedited and formatted. The final version may differ from this version.

Table 2: Hepatic BNIP3 mRNA expression after APAP overdose

	Real-time PCR (BNIP3:HPRT versus SAL in HIF-1α$^{+fl/+fl}$					
	SAL			APAP		
Mouse	**2h**	**6h**	**24h**	**2h**	**6h**	**24h**
HIF-1α$^{+fl/+fl}$	1.0 ± 0.02	1.0 ± 0.02	1.0 ± 0.1	0.72 ± 0.13	0.33 ± 0.04	0.4 ± 0.7[a]
HIF-1α$^{\Delta/\Delta}$	0.78 ± 0.1	0.77 ± 0.1	1.2 ± 0.24	2.1 ± 0.5[ab]	0.77 ± 0.26	0.32 ± 0.1[a]

HIF-1α$^{+fl/+fl}$ and HIF-1α$^{\Delta/\Delta}$ mice were treated with SAL or APAP then killed at 2, 6 or 24h. Real-time PCR was used to analyze liver tissue for expression of BNIP3 mRNA. For each sample, the copy number of BNIP3 was normalized to that of HPRT, then further normalized to SAL-treated HIF-1α$^{+fl/+fl}$ mice to account for variability in mRNA quantity at different time points. Data represents mean BNIP3:HPRT:SAL ratio ± SEM of n=3-6 animals. *a* Significantly different from SAL-treated mice of same genotype; *b* Significantly different from corresponding HIF-1α$^{+fl/+fl}$ mice.

JPET Fast Forward. Published on May 16, 2011 as DOI: 10.1124/jpet.111.180521
This article has not been copyedited and formatted. The final version may differ from this version.

Table 3: Hepatic PAI-1 mRNA expression after APAP overdose in HIF-1α$^{+fl/+fl}$ and HIF-1α$^{\Delta/\Delta}$ mice

	Real-time PCR (PAI-1:HPRT ratio) x 100					
	SAL			**APAP**		
Mouse	2h	6h	24h	2h	6h	24h
HIF-1α$^{+fl/+fl}$	1 ± 0.5	1.0 ± 0.5	0.03 ± 0.1	16 ± 7[a]	14 ± 7[a]	12 ± 4[a]
HIF-1α$^{\Delta/\Delta}$	0.1 ± 0.03[b]	0.2 ± 0.03[b]	0.6 ± 0.2	26 ± 20[a]	2.9 ± 1[b]	11 ± 5[a]

HIF-1α$^{+fl/+fl}$ and HIF-1α$^{\Delta/\Delta}$ mice were treated with SAL or APAP then killed after 2, 6, or 24h. Real-time PCR was used to analyze liver tissue for the expression of PAI-1 mRNA. For each sample, the copy number of PAI-1 was normalized to that of HPRT. Data represent mean of the PAI-1:HPRT ratio ± SEM of n=3-6. *a* Significantly different from SAL-treated mice of same genotype; *b* Significantly different from corresponding HIF-1α$^{+fl/+fl}$ mice.

JPET Fast Forward. Published on May 16, 2011 as DOI: 10.1124/jpet.111.180521
This article has not been copyedited and formatted. The final version may differ from this version.

Table 4: Cytokine concentrations in plasma of APAP-treated HIF-1α$^{+fl/+fl}$ and HIF-1α$^{\Delta/\Delta}$ mice.

	Plasma cytokine (pg/mL)			
	SAL		**APAP**	
Cytokine	**HIF-1α$^{+fl/+fl}$**	**HIF-1α$^{\Delta/\Delta}$**	**HIF-1α$^{+fl/+fl}$**	**HIF-1α$^{\Delta/\Delta}$**
IFNγ	15.9 ± 1.0	17.3 ± 1.4	17.4 ± 1.5	17.6 ± 0.5
IL-1β	6.1 ± 0.5	6.2 ± 0.3	6.9 ± 0.6	6.5 ± 0.5
IL-2	4.0 ± 0.4	3.8 ± 0.2	5.8 ± 0.9	4.4 ± 0.3
IL-4	4.8 ± 0.3	5.0 ± 0.5	4.5 ± 0.4	4.2 ± 0.3
IL-6	23.5 ± 3.0	27.8 ± 3.7	231 ± 45.1 [a]	38.2 ± 5.6 [b]
IL-10	10.9 ± 0.4	11.6 ± 0.4	14.0 ± 1.4	11.5 ± 0.2
IL-12 (p70)	14.8 ± 0.6	15.4 ± 0.2	14.6 ± 0.5	14.4 ± 0.3
KC (mIL-8)	49.8 ± 7.4	40.3 ± 8.0	573 ± 372 [a]	110 ± 25.5 [b]
MIP-1α	11.5 ± 0.5	12.1 ± 0.3	12.4 ± 0.7	12.0 ± 0.3
RANTES	28.5 ± 4.0	27.3 ± 1.5	52.9 ± 10.9 [a]	33.2 ± 3.2 [b]
TNFα	17.9 ± 0.4	18.4 ± 0.5	20.0 ± 1.0	18.3 ± 0.4
VEGF	19 ± 0.4	20.5 ± 0.6	19.1 ± 0.6	19.5 ± 0.6

HIF-1α$^{+fl/+fl}$ and HIF-1α$^{\Delta/\Delta}$ mice were treated with SAL or APAP, and plasma was collected 6h after administration and analyzed for cytokine concentrations using bead array. *a* significantly different from SAL-treated HIF-1α$^{+fl/+fl}$ mice; *b* significantly different from APAP-treated HIF-1α$^{+fl/+fl}$ mice.

Figure 1

JPET Fast Forward. Published on May 16, 2011 as DOI: 10.1124/jpet.111.180521
This article has not been copyedited and formatted. The final version may differ from this version.

A

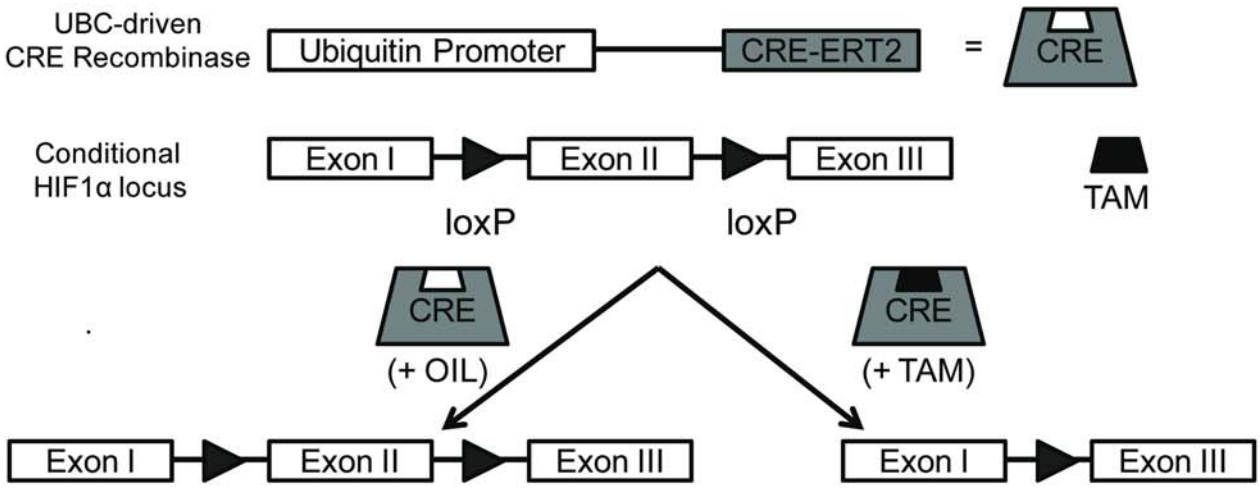

B

	Real-time PCR (HIF-1α:HPRT versus SAL-treated HIF-1α$^{+fl/+fl}$)			
Genotype	HIF-1α$^{+fl/+fl}$		HIF-1α$^{\Delta/\Delta}$	
Treatment	2h	24h	2h	24h
SAL	1 ± 0.04	1 ± 0.1	0.03 ± 0.002[a]	0.00055±0.0004[a]
APAP	2.3 ± 1.5[a]	437 ± 375[a]	0.03 ± 0.001[ab]	26 ± 12[a]

C

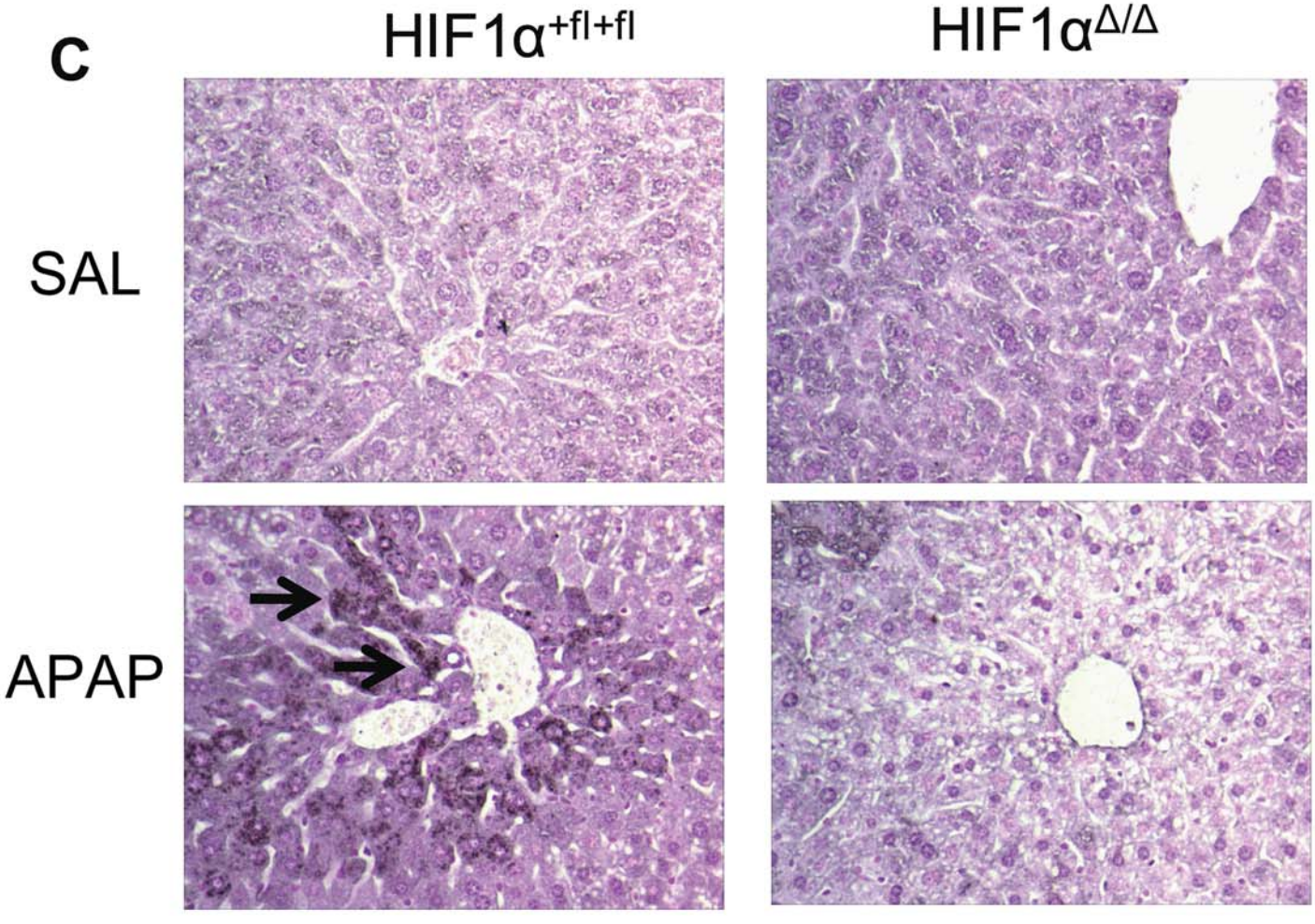

JPET Fast Forward. Published on May 16, 2011 as DOI: 10.1124/jpet.111.180521
This article has not been copyedited and formatted. The final version may differ from this version.

Figure 2

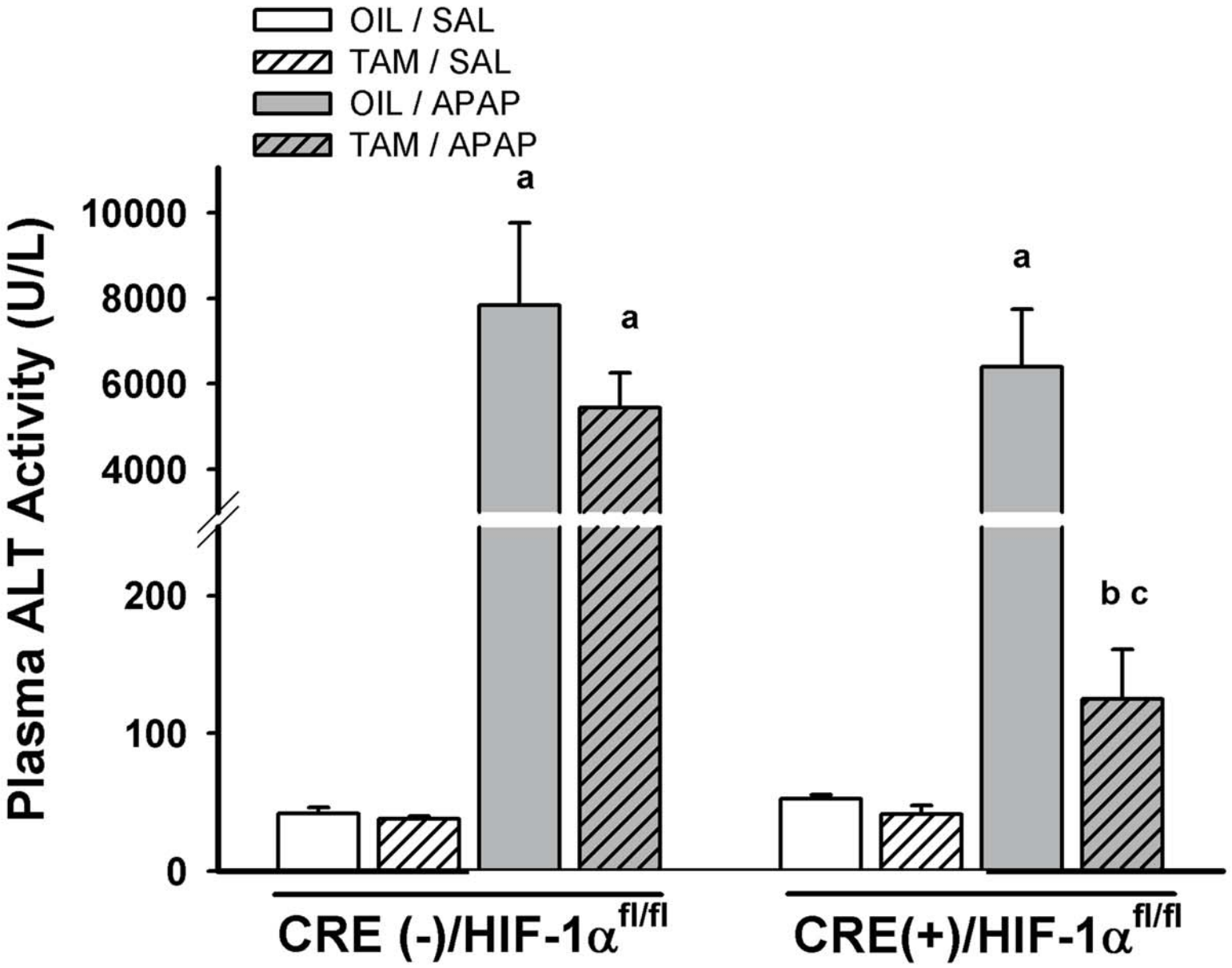

Figure 3

JPET Fast Forward. Published on May 16, 2011 as DOI: 10.1124/jpet.111.180521
This article has not been copyedited and formatted. The final version may differ from this version.

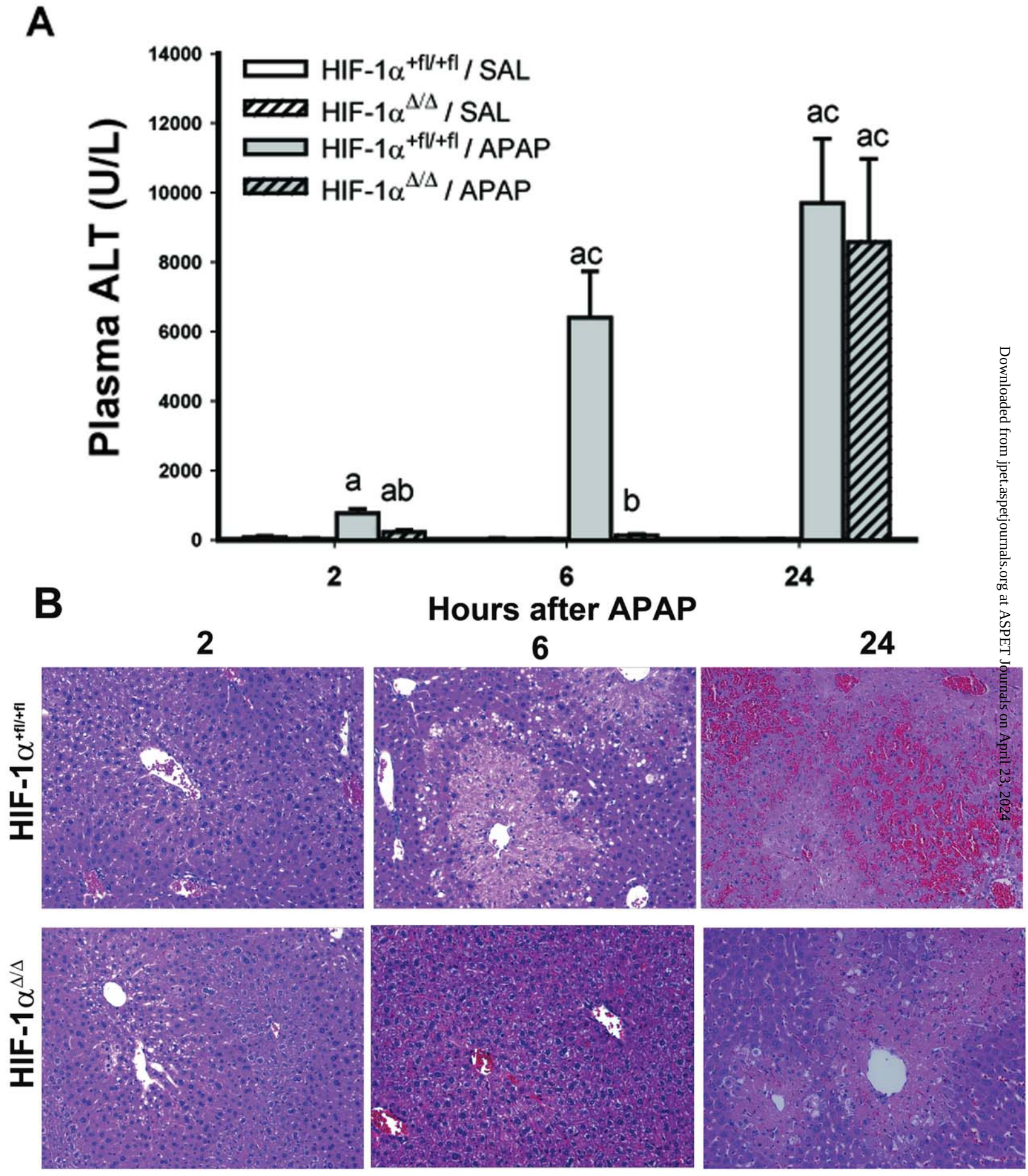

Figure 4

JPET Fast Forward. Published on May 16, 2011 as DOI: 10.1124/jpet.111.180521
This article has not been copyedited and formatted. The final version may differ from this version.

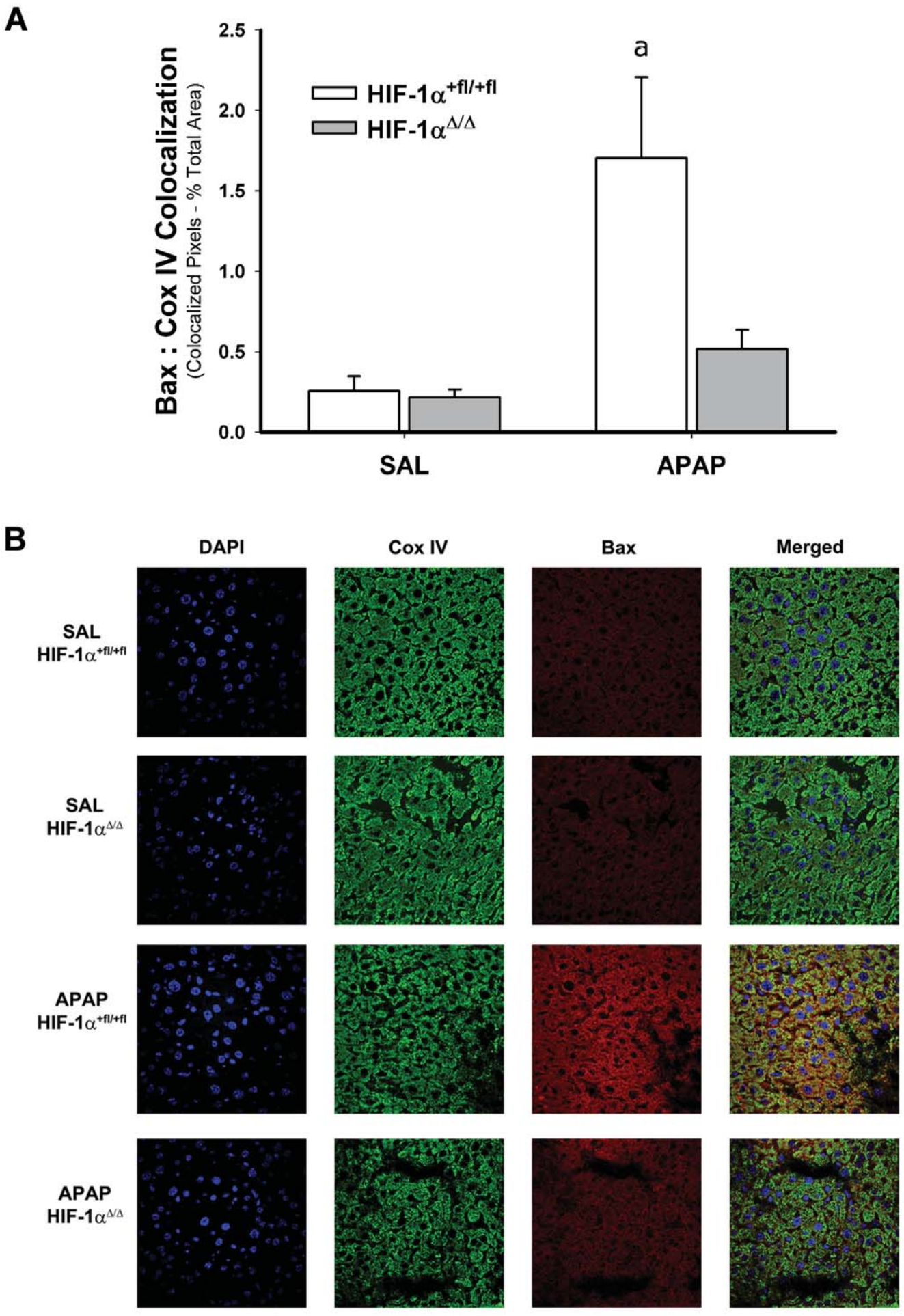

Figure 5

JPET Fast Forward. Published on May 16, 2011 as DOI: 10.1124/jpet.111.180521
This article has not been copyedited and formatted. The final version may differ from this version.

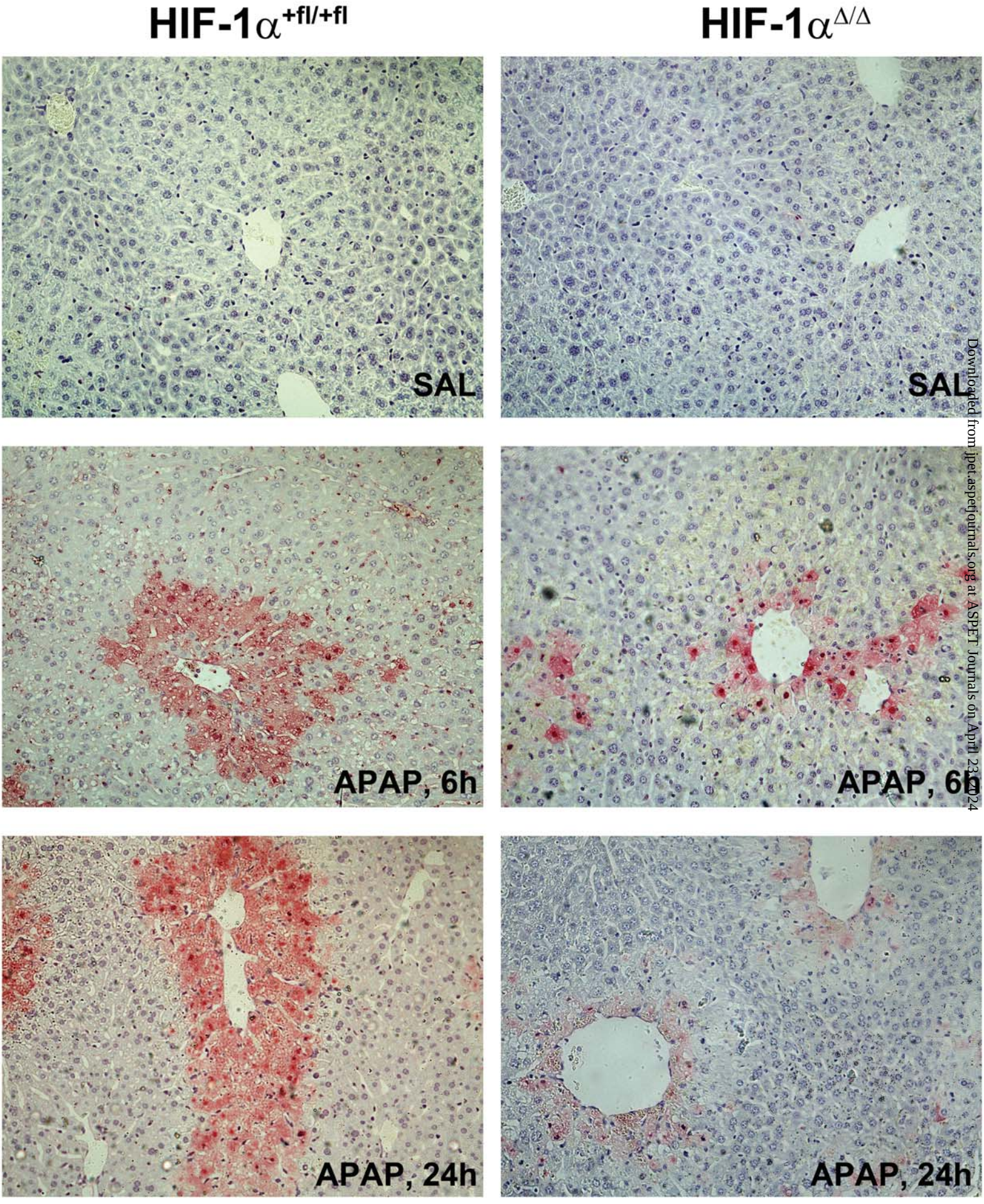

Figure 6

JPET Fast Forward. Published on May 16, 2011 as DOI: 10.1124/jpet.111.180521
This article has not been copyedited and formatted. The final version may differ from this version.

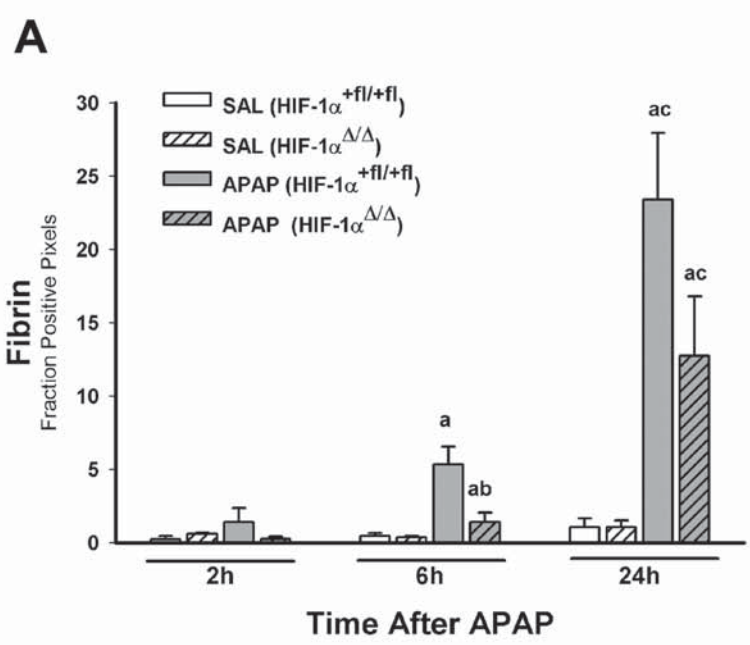

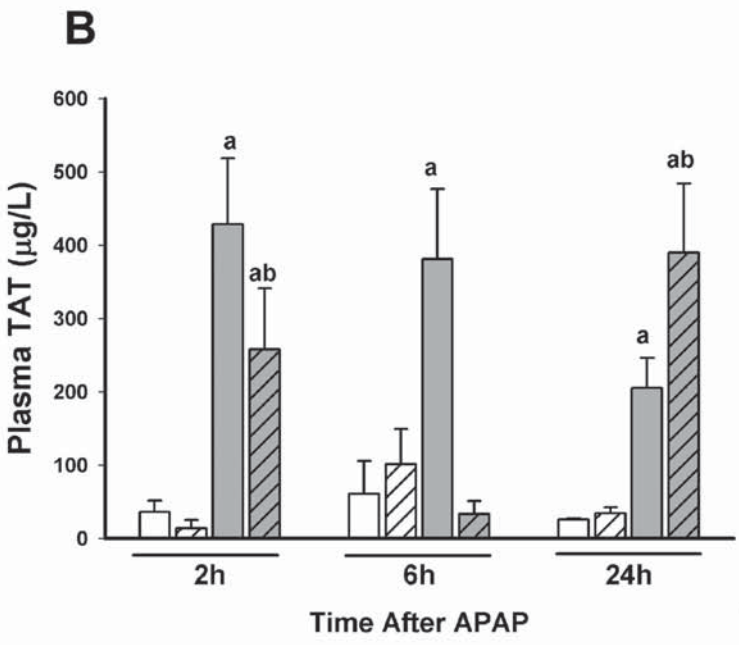

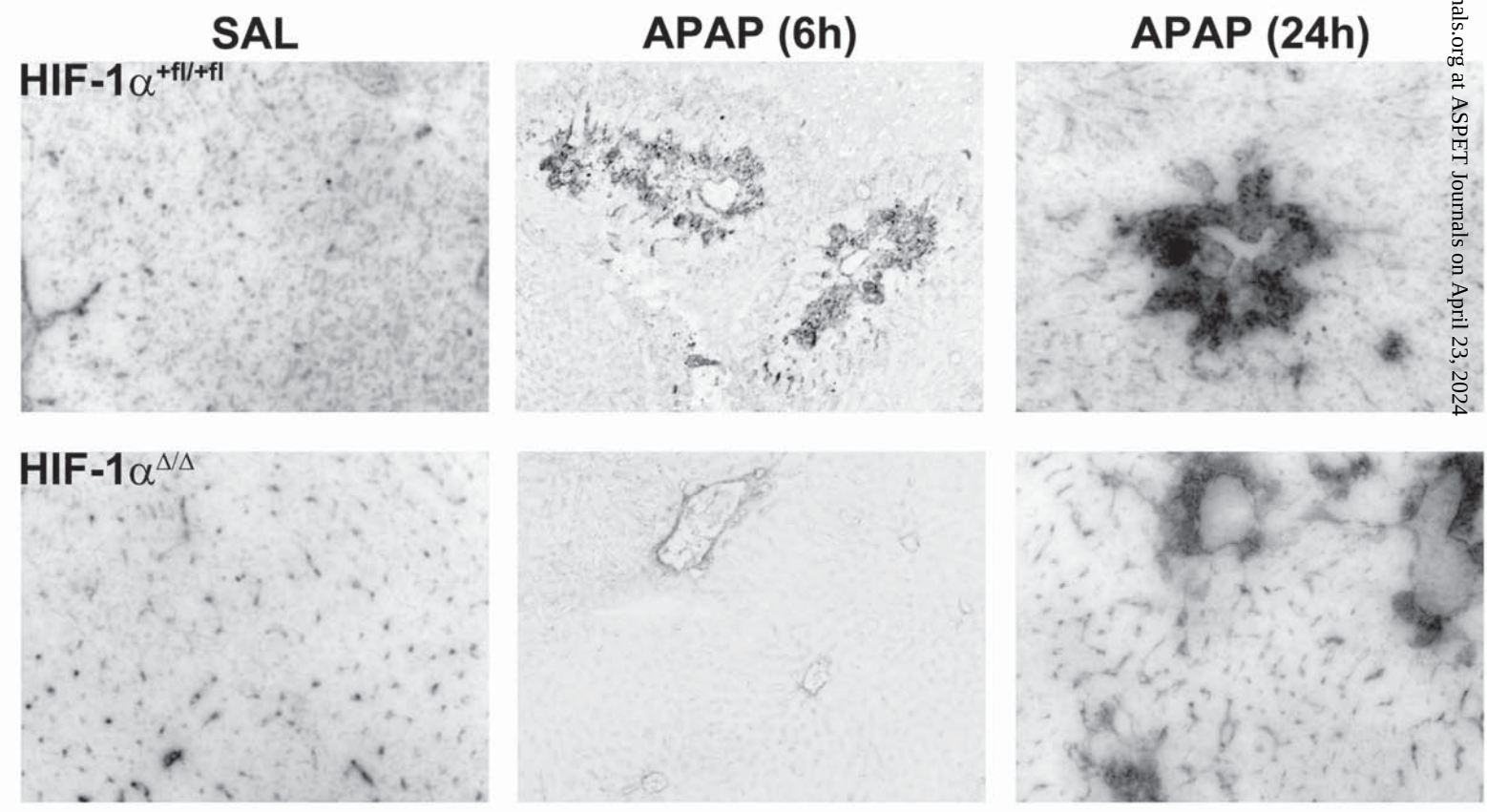

Figure 7

JPET Fast Forward. Published on May 16, 2011 as DOI: 10.1124/jpet.111.180521
This article has not been copyedited and formatted. The final version may differ from this version.

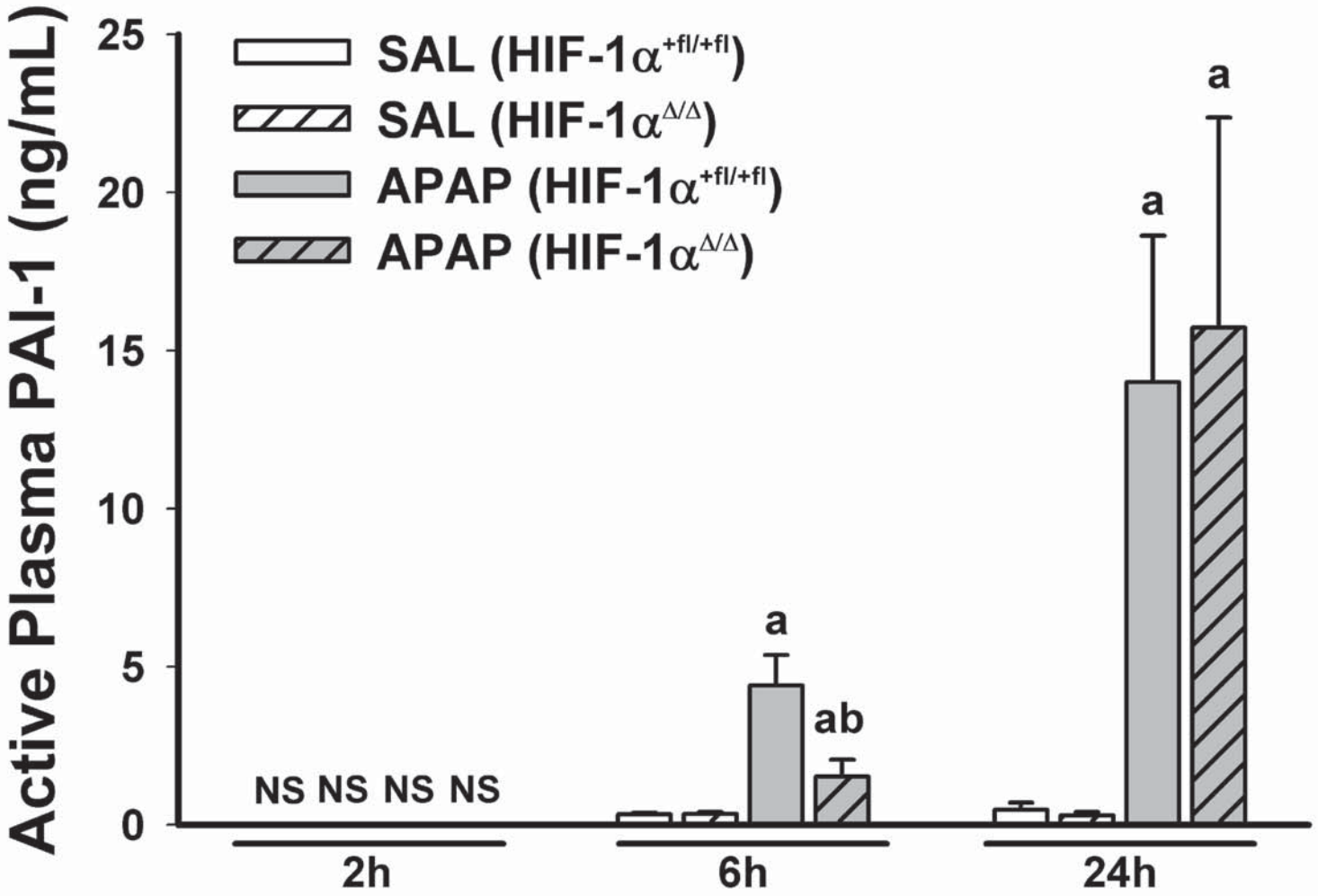

Figure 8

JPET Fast Forward. Published on May 16, 2011 as DOI: 10.1124/jpet.111.180521
This article has not been copyedited and formatted. The final version may differ from this version.

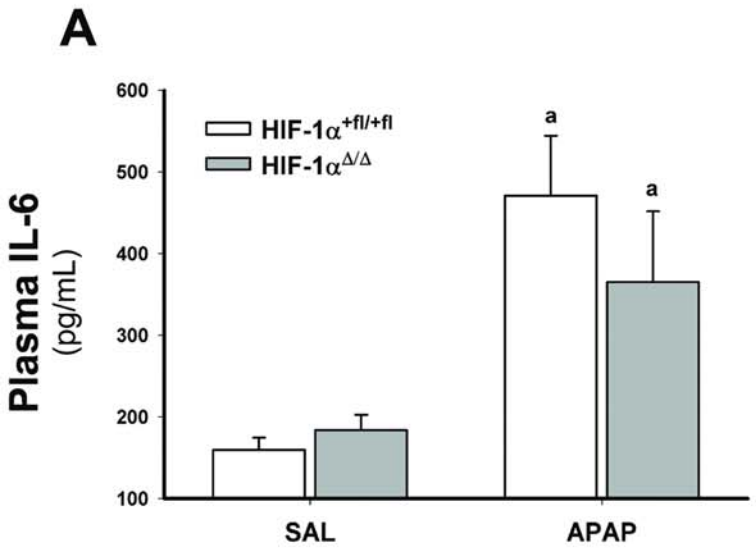

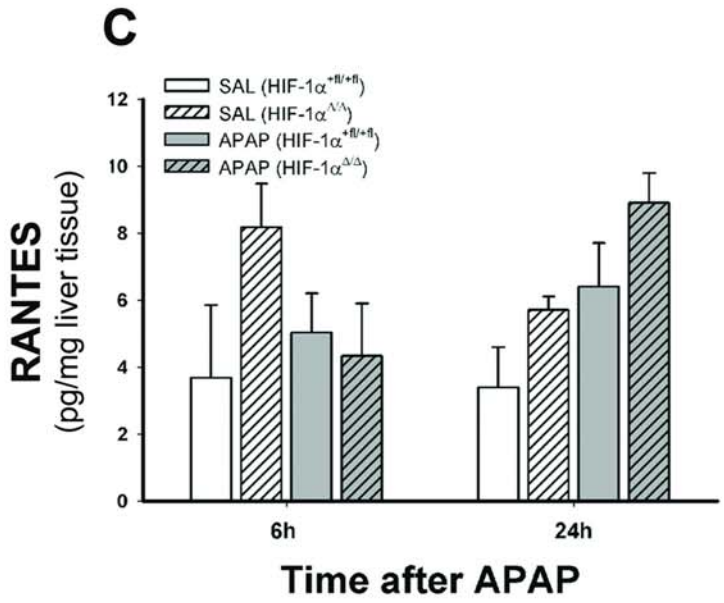

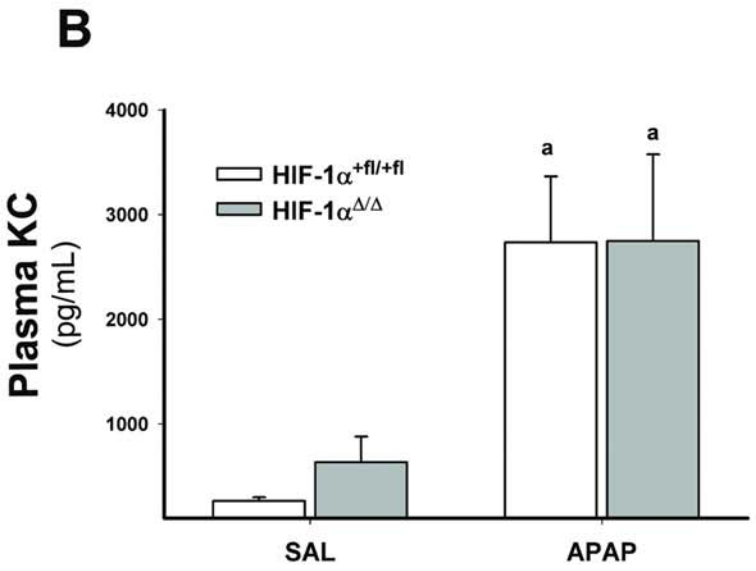

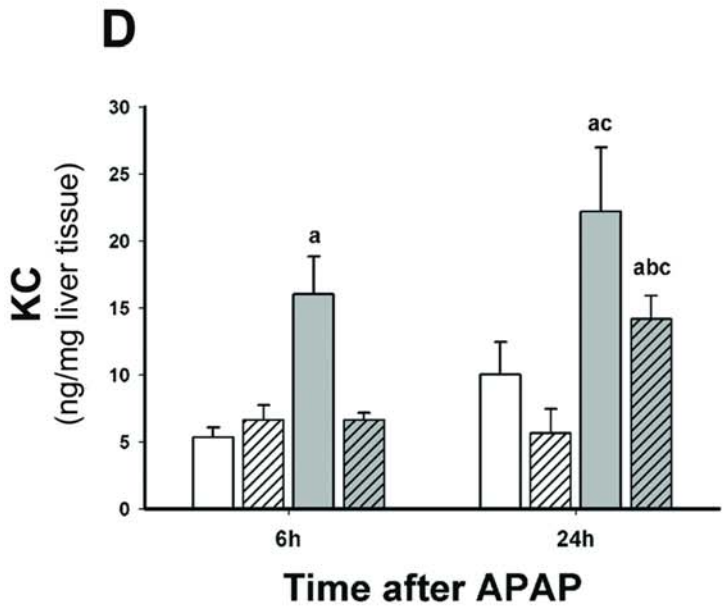

JPET Fast Forward. Published on May 16, 2011 as DOI: 10.1124/jpet.111.180521
This article has not been copyedited and formatted. The final version may differ from this version.

Figure 9